9. Langlois, G. E., J. E. Gullberg, and Theodore Vermeulen, *Rev. Sci. Instr.*, **25**, 360 (1954).
10. Leibson, Irving, E. G. Holcombe, A. G. Cacoso, and J. J. Jacmic, *A.I.Ch.E. J.*, **2**, No. 3, 300 (1956).
11. McDonough, J. A., W. J. Tomme, and C. D. Holland, *ibid.*, **6**, 615 (1960).
12. Scott, L. S., W. B. Hayes III, and C. D. Holland, *ibid.*, 4, 346 (1958).
13. Stiles, G. B., Dissertation, Texas A&M Univ., College Station (1964).
14. Trice, V. G., Jr., and W. A. Rodger, *A.I.Ch.E. J.*, **2**, 205 (1956).
15. Van Krevelen, D. W., and P. J. Hoftijzer, *Chem. Eng. Progr.*, **46**, 29 (1950).
16. Vermeulen, Theodore, G. M. Williams, and G. E. Langlois, *ibid.*, **51**, 85 (1955).
17. Walters, J. K., and J. F. Davidson, *J. Fluid Mech.*, 17, 321 (1963).

Manuscript received May 18, 1965; revision received September 23, 1965; paper accepted September 24, 1965.

A Computational Model for the Structure of Porous Materials Employed in Catalysis

RICHARD N. FOSTER and JOHN B. BUTT

Yale University, New Haven, Connecticut

A computational model for the structure of porous materials such as those employed in catalysis is proposed. The void volume within the solid is considered to be composed of two major arrays of pores, centrally convergent and centrally divergent, respectively, interconnected at specified intervals within the arrays. The exact shape of these arrays is determined uniquely from the volume-area distribution of the porous structure.

The model is applied to computation of counterdiffusional flux through a porous solid as measured in a Wicke-Kallenbach experiment. The effects of dead end pores and of mixing on the results are discussed, and comparison with experimental data reported for a particularly well-defined system is given.

The importance of internal or pore diffusion processes in catalysis has been recognized for a number of years. Various applications to problems of simultaneous diffusion and reaction have been detailed by many workers (*1*), and it has been shown that the process of mass transport within a porous solid is a highly complex one which is strongly affected by the nature of the porous structure itself. Most often these effects have been incorporated into an effective diffusivity definition which is then employed as a parameter in the solution of the normal diffusion equation; however, there are grounds for serious doubts as to whether the effective diffusivity approach alone can properly describe such mass transport processes.

Several attempts have been made to relate in quantitative fashion the effective diffusivity to properties associated with the structure of the porous matrix. Wheeler (*2*) approached the problem by assuming that the effective diffusivity of a gas in a porous material was proportional to the ordinary bulk diffusivity. The constant of proportionality was called the *labyrinth factor* or *tortuosity*. Hoogschagen (*3*) noted in his review of theories concerning tortuosity that various developments, particularly those of Bruggeman (*4*) and Maxwell (*5*), lead to somewhat different results. Further, actual measurements of tortuosity were not easily explained in terms of properties of the porous solid and the quantity could not be extrapolated reliably. The basic weakness of such theory resides in the fact that the effective diffusivity within a porous matrix is probably not directly proportional to the bulk diffusivity, but is a complex function of bulk diffusivity, Knudsen diffusivity, and the pore structure geometry.

A theory providing more detail results from the use of a macropore-micropore model, in which the solid is viewed as consisting of small, individual particles, each possessing a micropore structure, agglomerated into a pellet or tablet in which the macropore structure is formed by the process of manufacture. This model has been used in a considerable amount of work dealing with catalytic effectiveness and selectivity (*6, 7*), but the relationship of effective diffusivity to the individual pore structure is not defined by the model.

The point is that an overall description of the porous matrix cannot define pore structure effects; one must consider the transport process in individual pores and then assemble this into an appropriate overall description. The basis for this is provided by the analysis of Scott and

Dullien (8), who have presented the equations for mass transport by diffusion in cylindrical capillaries in which either or both Knudsen and bulk diffusion are important. Though individual pores may certainly not be cylindrical, this forms a convenient basis for study of the individual transport process, since postulation of more complex geometries will, in practice, require more information than is available. The transport equation, written in terms of mole fractions for one-dimensional diffusion in an ideal gas, has the differential form

$$N_A = -\frac{P}{RT}\left[\frac{1}{\frac{(1-\alpha y_A)}{\mathcal{D}_{AB}} + \frac{1}{D_{KA}}}\right]\frac{dy_A}{dx} \qquad (1)$$

or, on integration over L

$$N_A = \frac{P\mathcal{D}_{AB}}{RTL\alpha}\ln\left[\frac{(1-\alpha y_{A2}) + \mathcal{D}_{AB}/D_{KA}}{(1-\alpha y_{A1}) + \mathcal{D}_{AB}/D_{KA}}\right] \qquad (2)$$

A second, important result incorporated in the equations above is that the ratio of fluxes α is determined from the following relationship:

$$N_A\sqrt{M_A} + N_B\sqrt{M_B} = 0 \qquad (3)$$

in the absence of total pressure gradients. It has been shown (3) that this pertains to diffusion through porous materials when either Knudsen or bulk diffusion is controlling and in the general case when both are significant (12).

Wakao and Smith (9) have postulated the most detailed pore structure model to date. Using the results of Equations (1) and (3) to describe the transport process in individual pores, they derived an equation for the rate of mass transfer of gaseous material through a porous matrix. The approach is based on viewing the structure to consist of a random arrangement of micropores and macropores in which individual and series combinations of the two are considered. The transport equation resulting involves micropore and macropore porosities and average radii as parameters and the model appears to correlate the available experimental data on mass transport through solids well.

On closer examination, however, there are several disadvantages associated with the random pore model; it is assumed, for example, that volume and area void fractions are equal, that the statistical assembly within a unit cell is properly represented by the square of the area void fraction, that the diffusion within the solid may be represented as a one-dimensional process with equal lengths associated with each of the characteristic pore systems, and that properties such as porosity and average radius are single-valued functions of the pore size distribution. It is not our purpose here to become involved in a detailed criticism of this or other pore structure models, for no model can hope to be correct in every respect, but rather to develop from a somewhat different point of view a description of mass transport within porous structures which may circumvent in some measure the arbitrary nature of such previous work.

RELATIONSHIP OF POROUS STRUCTURE TO THE VOLUME-AREA DISTRIBUTION

An important question which arises in the study of pore structure is the relationship of such gross properties as surface area, porosity, and average radius to the volume-area, or pore size, distribution. As pointed out above, most previous approaches, at least implicitly, have assumed a unique relationship; the inaccuracy of this may be demonstrated by considering Equation (4) which relates the porosity to the characteristics of the pore size distribution.

$$\epsilon = \sum_i \frac{S_i}{4\Delta V_p} \qquad (4)$$

Thus there are many sets of ΣS_i for Equation (4) which result in identical values of porosity, and this quantity must be considered as a multivalued function of the pore size distribution. Similar results pertain for the other overall properties.

Differences in pore structure as reflected by the pore size distribution can affect the diffusional flux, and one of the major objectives of the present work has been the development of an approach to mass transport in porous solids which takes into account the specific nature of the volume-area distribution function. It is important to do this, since distribution data represent a considerable fraction of the information available to us concerning the properties of a porous structure.

GEOMETRICAL DESCRIPTION OF THE MODEL

In the present work, as in previous cases, it is assumed that the resistance to diffusion may be computed through construction of a suitable array of cylindrical pores. The tortuosity factor approach attempted to account for randomness and irregularities by use of a constant factor; Wakao and Smith postulated two major groups of pores with a third group formed by the coincidence of the original major groups. The present model also postulates two major arrays of pores. The hypothesized porous structure is divided into two halves, each a mirror image of the other. The entire pore volume of the model is made of two conical arrays, one of which is narrowest at the center of the solid, which will be called centrally convergent; the other is widest at the center, which will be called centrally divergent (see Figure 1). The centrally convergent array is the inverse of the centrally divergent array. The exact shape of these arrays is determined uniquely by the pore size distribution function of the porous structure by assigning the volume corresponding to a given radius to segments of the two arrays of that radius. Diffusional path lengths are normalized with respect to overall particle dimensions, so the two-pore combination is computationally equivalent to n centrally convergent and n centrally divergent pore arrays. The details of the methods for determination of the dimensions of the pore arrays are given subsequently.

It is obvious on examination of Equation (2) that the concentrations (mole fractions) of material diffusing through each of the arrays are functions of the initial con-

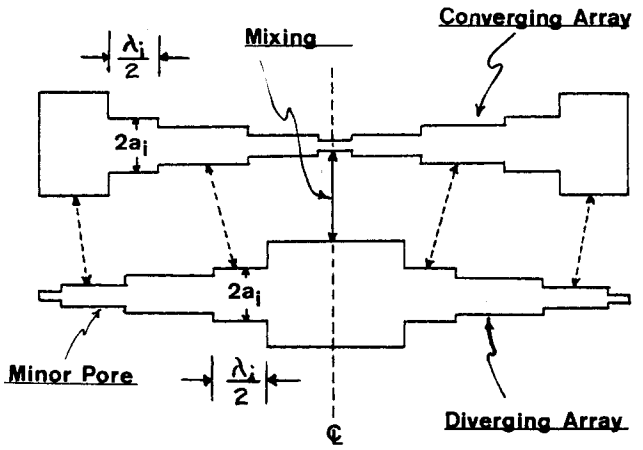

Fig. 1. Simplified geometric representation of the convergent divergent pore array.

centrations and the geometry of the individual segments of the array. More explicitly, the concentration drop over each segment will be different in the centrally convergent array than in the centrally divergent array due to the nature of the functional dependence of concentration on radius and length. This behavior is typical of the diffusion process as illustrated in Figure 2. It can be seen that the diffusion path for the one-volume element may be considerably different than for another, both starting at the same point A and ending at the same point B. Physically, the two-volume elements will mix at this point and then procede to the next labyrinth. Simulation of the diffusion process of Figure 2 may be completed, then, by providing for the mixing of concentrations at various points within the arrays. In the model this is accomplished by mixing the calculated concentrations within the arrays when the total lengths of the corresponding segments are the same. Various degrees of mixing may be provided for by relaxing the equality of length requirement to one of equality within a specified percentage range. This is represented in Figure 1 by the solid and dashed lines joining the two arrays.

We have to this point developed a model of porous structure which accounts in principle for both parallel and series resistances to diffusion, for mixing and for the multidimensional nature of the transport process, and which is uniquely determined by the observable properties of the solid as represented by a pore size distribution function. There is one quantity which is not specified by the pore size distribution, and therefore is not specified in the model: the fraction of total volume or of porosity inactive for transport. This volume is associated with blank or dead end pores and represents an infinite resistance to diffusion; diffusional fluxes computed by the model will be expected to be high if the total volume is assumed active for transport.

SPECIFICATION OF THE PORE ARRAYS

The range of pore radii which must be considered in establishing the two-pore array is defined explicitly, together with the corresponding volumes, by the pore size distribution function. To calculate the arrays required, we must compute the pore lengths which are to be associated with a given radius. In fact, a distribution of pore lengths for each radius must exist, and its approximate nature be found. This procedure will then define a set of lengths corresponding to the radius distribution function and the conical pore array will consist of a series assembly of many porous segments of known radius and length. These individual segments are called minor pores. From Equation (2) the concentration drop across each of these minor pores may be determined and, in summation, across the entire array (also termed a major pore). Since the radius is given directly by the pore size distribution, the specification of pore structure geometry required for the model is the length of each minor pore within the array.

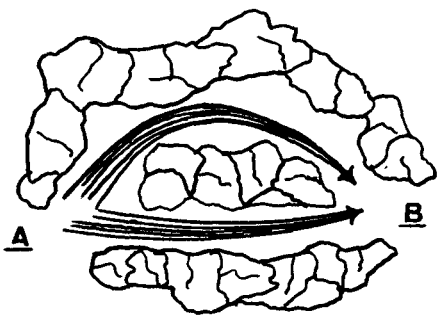

Fig. 2. Illustration of diffusion path and mixing in a pore labyrinth.

The total length of κ_i pores of radius a_i may be determined from the volume-area distribution, assuming cylindrical geometry, as

$$L_i = \kappa_i \lambda_i = \frac{v_i}{\pi a_i^2} \tag{5}$$

It is desired to calculate λ_i, which is normalized length, with respect to the overall particle dimension L_p to obtain an appropriate diffusion length associated with capillaries of radius a_i.

The equivalent lengths may be derived as follows. Consider two pores of radius a_i and a_{i+1}. It can then be shown that

$$dV_i = \int_{a_i}^{a_{i+1}} p(a)\, d \ln a \tag{6}$$

Geometrically, this volume, which corresponds to pores between radius a_i and a_{i+1}, is also given by

$$dV_i = \pi d(a_i^2 L_i) \tag{7}$$

By rearranging Equation (7) and by substituting Equation (6) for dV_i, one obtains

$$dL_i = d\left[\frac{p(a)\ln a}{\pi a^2}\right]_i \tag{8}$$

This represents the total length of all pores of radius a to $a + da$ on the pore structure. The total length of all pores of all radii in the pellet L_T is obtained from the integration of Equation (8) for all radii:

$$L_T = \int_{a_1}^{a_F} d\left[\frac{p(a)\ln a}{\pi a^2}\right] \tag{9}$$

where a_F is the final value of the radius included on the pore size distribution function.

A frequency distribution of lengths may be defined as the probability of finding a length associated with pores of radius between a and $a + da$ as related to the lengths of all pores in the structure. Thus

$$p(L_i) = \frac{dL_i}{L_T} = \frac{d\left[\frac{p(a)\ln a}{\pi a^2}\right]_i}{\int_{a_1}^{a_F} d\left[\frac{p(a)\ln a}{\pi a^2}\right]} \tag{10}$$

This probability is precisely the one required to determine the most probable diffusion path length or, equivalently, the normalized length, Thus

$$\lambda_i = p(L_i) Lp = \frac{d\left[\frac{p(a)\ln a}{\pi a^2}\right]_i}{\int_{a_1}^{a_F} d\left[\frac{p(a)\ln a}{\pi a^2}\right]} L_p \tag{11}$$

An example of such a distribution of normalized lengths is presented in Figure 3 for the pore size distribution presented in Figure 6 (Curve A).

APPLICATION OF THE MODEL; COMPUTATION OF FLUX-CONCENTRATION RELATIONSHIPS

We assume initially that the mole fractions of the two components, at opposite surfaces of the solid, are fixed at some known value. We also select arbitrarily a value of the diffusional flux.* For this combination of flux and initial concentration, a suitable arrangement of Equation (2) gives

* This value of flux, within the porous structure, must be related to the area of the total particle available for diffusion. This is simply the area of the pellet exposed multiplied by the surface porosity, defined as 2/3 of the volumetric porosity.

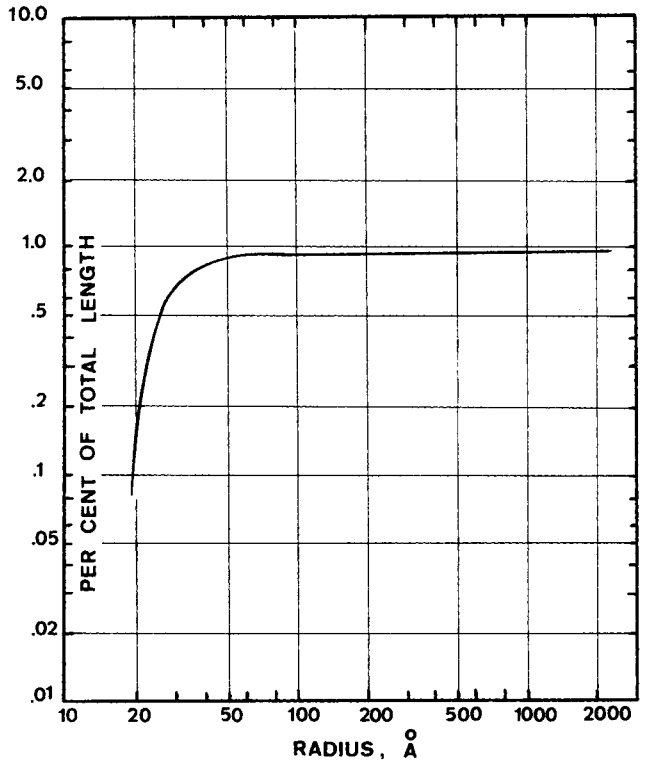

Fig. 3. Normalized length calculation for curve A of Figure 6.

maintained for the two components at opposite ends of a porous plug of the solid. These mole fractions are established by means independent of the diffusional transport within the solid, and therefore represent fixed end conditions to which the flux adjusts in steady state conditions. A second type of experiment is steady state diffusion between two infinite reservoirs in which the composition of the gases happens to correspond to the diffusional flux-concentration drop relationships imposed by the mass transport process itself. In this situation, the concentrations at the opposite surfaces are not externally and independently controlled.

In the particular experiment where the mole fractions are maintained near unity distinctions between the two as regards computation are not significant. Much experimentation has been reported in which mole fractions at the opposite faces have been different from unity; however, it is not clear whether this is the result of true independent control or of diffusional resistance in a fluid film or boundary layer adjacent to the solid surface. For this reason, the true nature of mass transport flux reported from such experimentation is somewhat obscure.

The algorithm described applies directly to the case in which surface compositions are externally controlled. It can be seen that computation for a nonexternally controlled composition is somewhat more complex, since these values must be fixed by the calculation. In such cases, it is assumed initially that pure components exist at opposite faces of the solid plug. The computation for a given flux is carried out for the total length of the two arrays for

$$y_{A_{i+1}} = -\frac{\left\{\left[(1-\alpha y_{A_i}) + \frac{\mathcal{D}_{AB}}{D_{KA_i}}\right]\exp\left[\frac{N_A RT\lambda_i\alpha}{P\,\mathcal{D}_{AB}}\right]\right\} - \left(\frac{\mathcal{D}_{AB}}{D_{KA_i}}+1\right)}{\alpha} \qquad (12)$$

The value of $y_{A_{i+1}}$ is the mole fraction at the end of the $i^{th}+1$ minor pore segment and the initial value for the next segment. Repeated application of Equation (12) to each minor pore provides the composition-length relationship associated with the assumed flux N_A.

While in any minor pore segment, a comparison of total length between centrally convergent and centrally divergent arrays is made, and the next composition calculation is carried out in the array of shorter length; thus both arrays are considered concurrently. When the two sections are of equal length (or within a specified fraction of each other), the compositions are averaged, or mixed, according to Equation (13).

$$y_{ave_{ij}} = \frac{y_{cc_i}\Delta V_{cc_i} + y_{cD_j}\Delta V_{cD_j}}{\Delta V_{cc_i} + \Delta V_{cD_j}} \qquad (13)$$

In this manner the computations are carried on stagewise to the center of the pellet, at which point the compositions in the centrally convergent and centrally divergent pore arrays are again mixed. The resulting composition is employed as the initial value for minor pores in both arrays for the second half—from the center to the face—of the pellet. The computation is then carried through the total length of the two arrays for one of the diffusing components. The correct flux is determined by comparing computed concentration at the surfaces with the known values with the use of a simple iterative technique.

BOUNDARY CONDITIONS

There are a number of ways in which the computation may simulate different experiments, corresponding to the manner in which one handles the boundary conditions of concentration at the surface of the solid. In the general Wicke-Kallenbach (*10*) type of experiment with binary gas mixtures, specified compositions or mole fractions are one of the diffusing components according to the algorithm. An initial value for the surface composition of the second component is readily established by

$$y_B = 1.0 - y_A \qquad (14)$$

The computation is now carried out in the opposite direction through the solid for the second component (B according to the nomenclature above), using y_B from Equation (14) as the composition at the entrance to the first minor pore segment of the two arrays. This will result in a new value of surface concentration for A and B at the opposite surface (where y_A was assumed to be unity initially), and the iteration is continued with this new concentration condition. When assumed and computed surface concentrations are in agreement, the calculation is completed, yielding surface concentrations and concentration drops across the solid which correspond to the flux assumed.

SIMPLIFICATION OF THE DISTRIBUTION

The whole of the volume-area distribution may be included in the determination of the minor pore lengths λ_i, but for the case where surface concentrations are fixed, it is possible to establish some guide lines which permit that portion of the distribution contributing only a negligible amount to the total flux to be eliminated from consideration. This can result in considerable savings in computation time. For a unity concentration drop, that portion of the volume-area distribution for which

$$\frac{1-\alpha y_{A2} + \mathcal{D}_{AB}/D_{KA1}}{1-\alpha y_{A1} + \mathcal{D}_{AB}/D_{KA1}} \approx 1 \qquad (15)$$

or

$$\frac{1+\mathcal{D}_{AB}/D_{KA1}}{(1-\alpha)+\mathcal{D}_{AB}/D_{KA1}} \geq 0.98 \qquad (16)$$

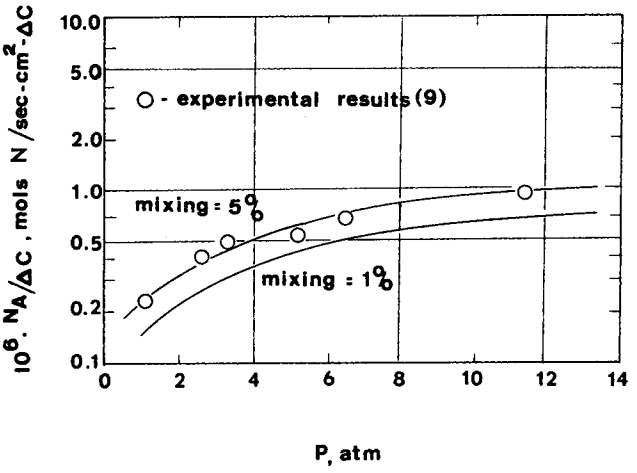

Fig. 4. Comparison of computed with experimental flux; data of Wakao and Smith (9); pellet *D*.

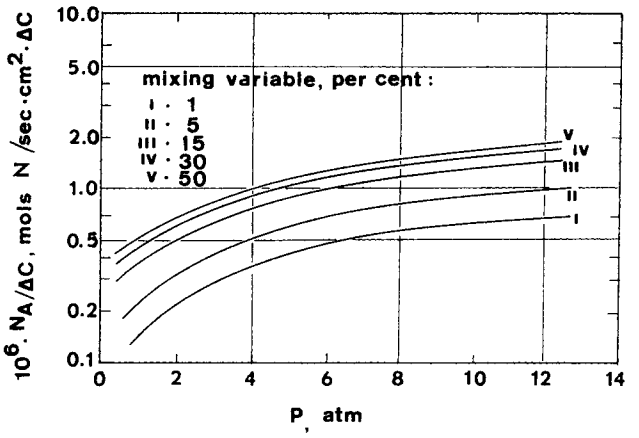

Fig. 5. Effect of mixing on diffusional flux computation.

contributes only a very small fraction (not greater than 2%) to the total flux and may be neglected. In terms of pore radius, this portion may be determined by solving for $(\mathcal{D}_{AB}/D_{KA1})$ from the inequality, making use of the well-known relationship

$$D_{KA1} = (9.7 \times 10^3)\, a_1 \sqrt{\frac{T}{M_A}} \qquad (17)$$

Another savings in computation can be effected in the representation of the pore size distribution by choosing radius increments such that the slope of the function is constant over the given increment. This will normally reduce the number of points required for the macropore region. In the computations reported here an increment of 5 Å. was used from the initial radius defined by Equation (17) up to 100 Å., 50 Å. from 100 Å. to 1,000 Å., and 500 Å. from 1,000 Å. to 10,000 Å. In this way the number of points to be considered was reduced from 2,000 to 60.

RESULTS—FLUX PREDICTIONS FOR A COUNTERDIFFUSION EXPERIMENT

A comparison of the flux computed by the convergent-divergent pore model with experimental values reported (9) for the counterdiffusion of helium and nitrogen through a well-characterized boehmite sample is given in Figure 4. The experimental data employed in the comparison resulted from what may be characterized as a well-defined Wicke-Kallenbach experiment, in which the mole fractions at opposite surfaces of the porous sample were maintained near unity in most cases.

If it is assumed that the microporous section of the catalyst particle is ineffective for diffusive transport (that is, the micropores are dead end pores), and if the overall porosity of the sample is taken as the porosity of the macropore section, since the micropores offer infinite resistance or act as a solid wall for diffusion, then the results fall below the measured data. If, in addition, the mixing criterion is relaxed to 5%, the predicted curve falls on top of the measured curve. It is believed that these variables, that is, a certain volume which is inactive for transport and an associated mixing effect, together form a more plausible explanation of the phenomenological effects than has heretofore been presented.

THE EFFECT OF MIXING

The effects of an important variable, the degree of mixing, are suggested in Figure 4. For the purpose of demonstrating the magnitude of the dependence of flux on the degree of mixing, in Figure 5 are presented computed results for the sample of Figure 4. The mixing variable is represented by the restriction on the agreement between total lengths of minor pore segments before mixing between the two arrays is permitted. When this restriction is relaxed to the vicinity of 30% (curve *IV* of Figure 5), mixing occurs at the end of almost every minor pore segment in this sample and further relaxation of the length restriction has only small effect. Increasing the degree of mixing always results in an increase in flux due to the higher average concentrations incident within the pore structure. In the example the possible effect of mixing is large: the flux differs by a factor of almost two between the extreme cases. Further generalization concerning the effects of mixing is not warranted, since these results are dependent on the nature of the volume-area distribution involved. (For example, Figure 5 indicates that mixing has little effect on the shape of the flux-pressure curve; this is not a general result.)

DIFFUSIONAL TRANSPORT AND THE VOLUME-AREA DISTRIBUTION

In a previous section it was shown that porosity and other overall properties of porous structures are not unique functions of the volume–area distribution and that any computational representation of porous materials

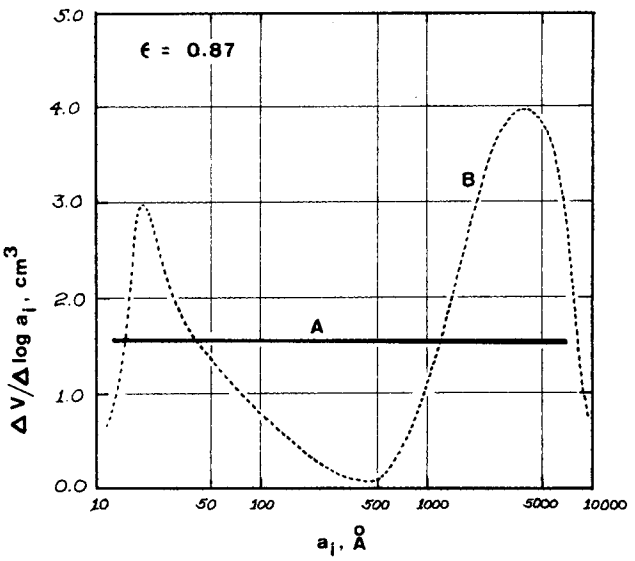

Fig. 6. Volume-area distributions, porous structures of equivalent porosity.

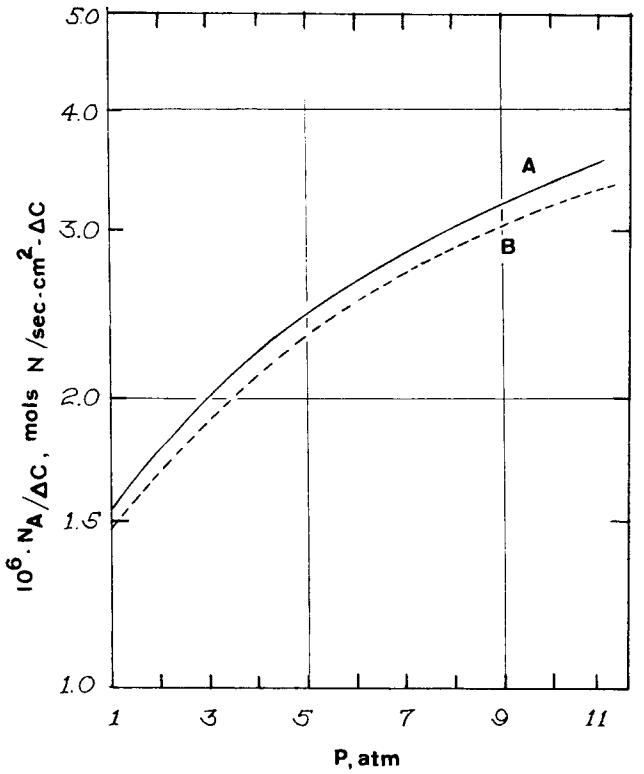

Fig. 7. Computed fluxes for two porous structures of equivalent porosity.

should accordingly be dependent on this distribution. In Figure 6 are given two volume–area distribution curves for porous materials. These distributions vary in their shapes, but yield identical values of porosity. The diffusional flux computed with the helium–nitrogen system at 297°K. under otherwise identical conditions for the two cases is given in Figure 7. The difference is a function of pressure and is about 5% of the total flux over the range of pressures for the illustration. The magnitude can be much greater than this, of course, depending on the distribution functions, gaseous system, temperature, and pressure. However, generalization is difficult owing to the number of parameters involved.

SUMMARY

In this discussion and initial testing of the convergent-divergent pore array model, we have attempted to establish that the approach accounts properly for the major variables involved in diffusional transport through porous structures—the relationship to the volume-area distribution, the importance of mixing or multidimensional transport paths, and the effects of dead end pores on observed flux. It is apparent that the latter two processes cannot be determined quantitatively from computational detail or from experimental data other than diffusional flux through porous structures under a very wide range of conditions. While the overall description of diffusion based on models employing gross properties such as porosity leaves much to be desired, the results of the present work indicate that some of the *individual* factors involved, such as mixing, may be well correlated on this basis. The data required to establish these relationships quantitatively, however, do not exist. Thus it is most important to obtain information on diffusional flux through porous structures of known properties by well-defined experiments over the widest available range of conditions. Application of the proposed pore structure model to the interpretation of these data will be given in a future report.

ACKNOWLEDGMENT

The authors are indebted to Harding Bliss for his many helpful comments and suggestions. This research was supported by the National Science Foundation.

NOTATION

a = pore radius, cm.
$\mathcal{D},D$ = diffusivity, sq. cm./sec.
L = capillary length, cm.
M = molecular weight, g./g.-mole
N = flux, moles/(sq. cm.)(sec.)
n = exponent in Equation (17)
P = pressure, atm.
p = probability
R = gas constant = 82.06, l. atm./(mole)(°K.)
S = slope of pore size distribution function
T = temperature, °K.
ΔV = capillary volume, cc.
v = volume of a pore, cc.
x = length coordinate in a pore, cm.
y = mole fraction

Greek Letters

α = $(1 - \sqrt{M_A/M_B})$
ϵ = porosity
κ = number of pores
λ = normalized pore length or length of a minor pore

Subscripts

A = component A
AB = mixture of A and B
$A1$ = A at face 1 of pellet
$A2$ = A at face 2 of pellet
A_i = A at interior pore i in the pellet
avg = average
b = pore length and volume for a particular radius as calculated by Equation (15)
B = component B
CC = centrally convergent array
CD = centrally divergent array
CC_i = centrally convergent array at pore i
CD_j = centrally divergent array at pore j
i = pore i in array
j = pore j in array
$KA1$ = Knudsen diffusion coefficient in smallest capillary considered in the distribution
P = entire catalyst particle
T = total void volume of particle
1 = smallest capillary considered in the distribution

LITERATURE CITED

1. Satterfield, C. N., and T. K. Sherwood, "The Role of Diffusion in Catalysis," Addison-Wesley, Reading, Mass. (1963).
2. Wheeler, A., "Catalysis," P. H. Emmett, ed., Vol. II, Reinhold, New York (1956).
3. Hoogschagen, J., *Ind. Eng. Chem.*, **47**, 906 (1955).
4. Bruggeman, D. A. G., *Ann. Phys.*, **24**, 636 (1935).
5. Maxwell, C., "Treatise on Electricity and Magnetism," Vol. I, Oxford Univ. Press, England (1873).
6. Carberry, J. J., *A.I.Ch.E. J.*, **8**, 557 (1962).
7. ———, *Chem. Eng. Sci.*, **17**, 675 (1962).
8. Scott, D. S., and F. A. L. Dullien, *A.I.Ch.E. J.*, **8**, 293 (1962).
9. Wakao, Noriaki, and J. M. Smith, *Chem. Eng. Sci.*, **17**, 825 (1962).
10. Wicke, E., and R. Kallenbach, *Kolloid Z.*, **97**, 135 (1941).
11. Mischke, R. A., and J. M. Smith, *Ind. Eng. Chem. Fundamentals*, **1**, 288 (1962).
12. Dullien, F. A. L., and D. S. Scott, *Chem. Eng. Sci.*, **17**, 771 (1962).

Manuscript received February 3, 1965; revision received September 30, 1965; paper accepted October 4, 1965. Paper presented at A.I.Ch.E. San Francisco meeting.